Journal of Fluorescence, Vol. 6, No. 1, 1996

Extrinsic Fluorescence Probe Study of Human Serum Albumin Using Nile Red

Daniel M. Davis[1] and David J. S. Birch[1]

Received December 18, 1994; accepted December 7, 1995

Nile red bound to human serum albumin (HSA) shows an order of magnitude increase in the probe's fluorescence intensity. Here, we report on the fluorescence characteristics of the probe–protein complex in Trizma buffer (pH 7.1), urea, guanidine hydrochloride, and AOT/isooctane/buffer reverse micelles using both steady—state and time-resolved fluorescence techniques. With a view to illustrating the use of extrinsic probe fluorescence spectroscopy in protein research, we demonstrate that protein unfolding can be observed through measurements of the probe's time-resolved anisotropy and steady-state fluorescence spectrum. Moreover, this shows that thermal unfolding is fundamentally different from using denaturant, with respect to changes in both the nanosecond diffusional rotation of the probe at intermediate stages and in the denatured protein's structure. Also, the large Stokes shift of Nile red allows the changes in the environment of the probe–protein complex in reverse micelles of varying waterpool size to be easily identified in the steady-state fluorescence. This was not seen in earlier work exploiting the intrinsic tryptophan fluorescence of HSA and further demonstrates the complementary information that extrinsic fluorescence probe studies can offer protein science. We discuss the complex acrylamide quenching characteristics of Nile red bound to HSA in terms of the possibility of at least two binding sites for the probe and the effect of acrylamide on the probe–protein structure at very high quencher concentrations.

KEY WORDS: Nile red; human serum albumin; fluorescence spectroscopy; protein dynamics; protein structure; protein unfolding.

INTRODUCTION

Experimental approaches to understand protein structures and dynamics are very wide ranging indeed.[1] However, time-resolved fluorescence measurements are not as commonplace within the protein research community as perhaps could be expected, given the valuable information that can be retrieved regarding both the protein structure and its nanosecond diffusional motions (e.g., Ref. 2). This is due to at least three reasons. First, the photophysics of the intrinsic fluorophore tryptophan is complicated, and even after many years of study the origin of its fluorescence decay is ambiguous.[3] This makes the interpretation of changes in the fluorescence lifetime decay all the more difficult to relate to physical changes in the probe's environment. Also, most proteins contain more than one tryptophan residue, which may lie in very different types of environment, further complicating the fluorescence decay.[4] Third, the collection time for an amount of data suitable for analysis by the various complex models is often in the range of hours. This means that faster processes such as protein folding cannot be easily observed through time-resolved fluorescence via stop-flow techniques, but only by studying the protein fluorescence under partially denaturing conditions,[5] which may or may not correspond to interme-

[1] Department of Physics and Applied Physics, University of Strathclyde, John Anderson Building, 107 Rottenrow, Glasgow, G4 ONG, UK.

1053-0509/96/0300-0023$09.50/0

diates in the folding transitions. However, it should be noted that there are many cases where steady-state fluorescence measurements including anisotropy data can rapidly give valuable information regarding protein folding transitions, such as the recent work by Beechem *et al.*[6]

Recent trends in the development of fluorescence spectroscopy and other biotechnological advancements are overcoming the above limitations. For example, the use of multiplexing electronics in data acquisition, can reduce the data collection time (and help overcome the "pile-up" problem), simultaneously obtaining a global fluorescence contour of wavelength, lifetime, and anisotropy.[7] Models for the global analysis of the fluorescence data have also been developed to allow the maximum amount of information to be retrieved.[8] Also, site-directed mutagenesis can place a single tryptophan probe in a desired location and/or replace unwanted tryptophan residues with tyrosine or phenylalanine (hopefully not distorting the protein structure in doing so).[5] However, to allow complicated global analysis of the fluorescence data, very accurate measurements must be made. In practice, the accuracy of the fluorescence decay data collected relies on the absence of systematic errors (e.g. instabilities of the excitation source, detection of scattered excitation) and the fluorescence being accumulated solely from the probe intended. Unfortunately, the fluorescence of tryptophan occurs in the wavelength region 310–350 nm with a small Stokes shift and is often obscured by other elements of the sample also fluorescing in that region and by strongly scattered excitation.

Our previous work using reverse micelles to investigate the effects of compartmentalization of proteins gave results which suggested the concept of protein compartmentalization aiding the process of folding by encouraging the correct protein structure to form as well as preventing protein aggregation.[9,10] To determine if this effect is static or dynamic in nature, it is necessary to carry out time-resolved fluorescence quenching measurements. However, this has proved difficult, because the surfactant used, namely, dioctyl sodium sulfosuccinate (AOT), or impurities within the commercially available sample fluoresce in the same wavelength region as the tryptophan probe with similar lifetime decay components that are quenched by carbon tetrachloride at rates indistinguishable from that of the tryptophan. Thus, with a view to overcoming this problem, we have bound the extrinsic fluorescent probe, 9-diethylamino-5*H*-benzo-[α]phenoxazine-5-one (Nile red), onto the protein used, human serum albumin (HSA). This is just one example of how the use of extrinsic fluorescent probes can increase the benefit of fluorescence spectroscopy for studying protein structure and dynamics. The main advantages of using an extrinsic probe is that the fluorescence emission and excitation can be chosen not to coincide with that of other molecules present, and the data collection time can be reduced, due to the higher quantum yield of the probe and the use of more intense laser sources at longer wavelength. A longer wavelength probe also reduces the Rayleigh scattered excitation. The main disadvantages of using an extrinsic probe is that the effects of the bound probe on the protein structure and dynamics are usually unknown, and often there are several binding sites on each protein molecule, again making the origin of the fluorescence decay components complex.

Nile red was first developed for use as a laser dye in the mid 1970s.[11] It has since been used in various experiments in its capacity to stain selectively nonpolar droplets or lipid molecules[12,13] and recently as a probe of hydrophobic protein surfaces.[14–16] The probe is nonionic, noncovalently binds to protein surfaces, and the large Stokes shift in its emission makes it particularly useful in observing changes in protein structure. It is also fairly insoluble, with its fluorescence almost fully quenched in aqueous solution. As expected, its fluorescence emission peak wavelength shifts to the red end of the spectrum in more polar environments (e.g., 642 nm in methanol and 615 nm in acetone).[15]

Sackett and Wolff showed that Nile red can be used as a probe of hydrophobicity for many proteins such as β-lactoglobulin and bovine albumin and that the dye is photostable, with its fluorescence unaffected by a pH between 4.5 and 8.5, and has a high quantum yield.[15] The same group subsequently reported a study of the hydrophobic surfaces of tubulin using both time-resolved and steady-state fluorescence of Nile red.[16] They report a biexponential fluorescence decay with components of 4.5 and 0.6 ns and conclude that there are two binding sites on the tubulin dimer, the more hydrophobic site being located in the region of subunit–subunit interaction (to account for fluorescence changes upon dilution). The more polar site was ascribed to the 0.6-ns component, as its fluorescence occurs at 665 nm, whereas the other component occurs at 623 nm. Also, they found the rotation of the short-lifetime component to be fast relative to the other. In contrast, however, the more polar site of Nile red was found to be virtually unquenchable by acrylamide, whereas the more buried site was statically quenched. More recently, Greenspan and Lou have studied the changes in the fluorescence of Nile red bound to native and oxidized low-density lipoprotein (LDL).[17] These previous studies are concerned

largely with characterization of the probe and its interactions with the protein through measurements of the fluorescence decay.

In this work we look at the example of Nile red bound to HSA and show how the fluorescence characteristics of the probe–protein complex varies in buffer, denaturant, and reverse micelles. The changes in fluorescence measurements, using both steady-state and time-resolved techniques in these different media, are related to the corresponding variation in protein behavior. In particular, time-resolved anisotropy measurements show how the rotational freedom of the probe varies in these different environments, providing information on the changing protein dynamics. This is complementary to quenching studies using acrylamide, which can show how the relative exposure of the probe varies, giving information on the changing protein structure. This builds on the previous work mentioned above, by demonstrating how interesting variations in both protein structure and protein nanosecond dynamics can be observed through appropriate experiments exploiting extrinsic probe fluorescence in different media. As developments in the techniques and instrumentation for fluorescence spectroscopy continue at a rapid pace, it is likely that the protein research community will become increasingly more aware of the uses of extrinsic fluorescence probe spectroscopy.

MATERIALS AND METHODS

HSA (essentially fatty acid and globulin free) and Nile red were used as received from Sigma and Aldrich, respectively. A stock solution of concentrated Nile red in dimethyl sulfoxide (DMSO) was prepared and kept at −20°C. Solutions of the probe–protein complex were prepared as required such that there was about one Nile red molecule per five protein molecules present, and the overall protein concentration for all experiments was about 1 mg/ml. The overall concentration of DMSO in all solutions was 0.04%, by volume, which corresponded to a maximum of 1.4% in the aqueous phase of reverse micelles. Trizma buffer (from Sigma), prepared using purified water, was used throughout all the experiments reported here, at pH 7.1, concentration 0.05 *M*, and ionic strength 0.1 *M*. The far-UV circular dichroism of HSA and the Nile red/HSA complex was measured in Trizma buffer using a Jobin Yvone Dichrograph CD6.

AOT and HPLC-grade isooctane were used as received from Aldrich and Romil, respectively, and a stock solution of 0.25 *M* AOT/isooctane was prepared. Reverse micelle solutions were then prepared by direct injection of the aqueous solution into the surfactant/hydrocarbon mixture using a Hamilton syringe. Generally, reverse micelles were initially formed at low waterpool sizes by injection of protein solution, and then swollen with subsequent aliquots of pure buffer. Hexadecyltrimethyl ammonium chloride (CTAC) was used as received, as a 25% solution in water from Fluka, and subsequently mixed with isooctane as appropriate. Concentrations of protein solution within the micellar system were such that multiple occupancy would be statistically unlikely with at least five reverse micelles per protein present. All experiments were performed at room temperature unless stated otherwise.

Time-resolved fluorescence measurements were made using the technique of single-photon timing. The excitation source was a nitrogen-filled coaxial nanosecond flashlamp,[18,19] with wavelength selection obtained using a Kratos GM-200 double monochromator with a 20-nm bandpass. Fluorescence emission was selected by a Schott cutoff filter and detected using a photomultiplier tube. In order to maximize the throughput of light, excitation was obtained using the bright nitrogen line at 358 nm, with emission selected by a 400-nm cutoff filter. Anisotropy measurements were obtained using Glan–Thompson polarizers, with emission at each polarization being detected alternately at 1-min intervals by automated rotation of the polarizer. All data analysis was performed with reconvolution using the IBH software library. The goodness of fit is represented by the normalized χ^2 and errors quoted are two standard deviations.

RESULTS AND DISCUSSION

The absorption of Nile red in buffer solution (pH 7.1) is centered around 575 nm, while that of Nile red bound to the protein is centered around 580 nm and of narrower width. Nile red/DMSO in aqueous solution has its peak emission wavelength around 655 nm, while binding to HSA blue-shifts the peak to about 639 nm and increases the emission intensity by approximately 20 times. The emission wavelength shift of the probe upon binding to the protein shows that it is bound to a hydrophobic region of the protein matrix. This can be expected from previous studies of Nile red/protein complexes.[15]

Stability of the probe/protein complex was also good, as expected after Sackett and Wolff[15] demonstrated binding of the probe to bovine serum albumin.

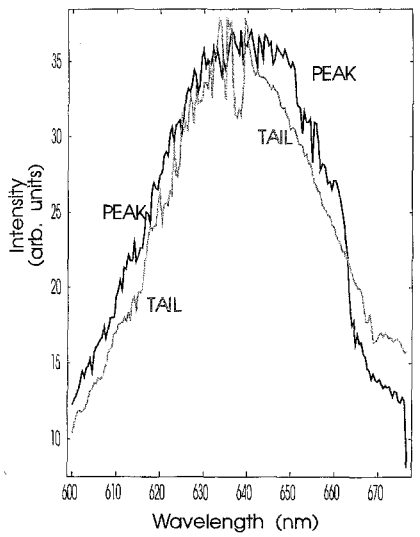

Fig. 1. Time-resolved emission spectra of Nile red bound to HSA in buffer (pH 7.1).

In fact, after mixing HSA and Nile red (by direct injection of each solution), the fluorescence intensity rapidly increases, taking around 5 min to reach its maximum, after which it is quite stable, decreasing only 5% in 7 h. It should be noted, however, that Nile red was not found to bind strongly to all proteins. For example, very little binding was found to occur with proteins such as lysozyme, which show little hydrophobic character. This was also reported by Sackett and Wolff.[15]

The results reported above demonstrate the appropriate use of Nile red bound to HSA, as determined for Nile red bound to other proteins in a similar fashion by Sackett and Wolff.[15] Although previous studies of Nile red/protein complexes failed to determine the effect of the bound probe on the protein's native structure, in the present work, the far UV circular dichroism of HSA in Trizma buffer was found to be unchanged in the presence of Nile red (and the appropriate small quantity of DMSO) at the concentrations used in the experiments to be described. This implies that the binding of Nile red to HSA does at least not substantially alter the native secondary structure of the protein in aqueous solution.

While the fluorescence from aqueous Nile red was too weak to resolve in time, the fluorescence decay of the bound probe was found to fit best to a function with three decay components, of 1.0 ± 0.1 ns (29%), 4.1 ± 0.1 ns (38%), and 9.6 ± 0.2 ns (33%). The origin of this multiexponential decay is not obvious. As discussed above, the lifetime components of 0.6 and 4.5 ns for Nile red bound to tubulin were assigned to excited states of the probe located in distinct binding sites.[16] Thus, to determine if the lifetimes of Nile red bound to HSA could be assigned to different binding sites, the time-resolved emission spectra of the probe/protein complex was measured.

Figure 1 shows the emission spectra taken at the peak and tail of the fluorescence decay to distinguish differences in the emission spectrum of the different lifetime components. It should be noted that the emission spectrum from the peak of the fluorescence decay also contains some scattered light from the 590-nm nitrogen line present in the flashlamp profile.[19] However, there is no evidence of a shift in the emission spectrum taken from the tail of the decay relative to that from the peak. This implies that the components of the decay cannot be located in substantially different environments within the protein structure. That is, if there are different binding sites of the probe within the HSA matrix, these cannot be of particularly distinct polarities.

Figure 2 shows the steady-state acrylamide quenching of Nile red bound to HSA in buffer presented as a Stern–Volmer plot.[20] There is an obvious upward deviation from a straight line at concentrations of acrylamide greater than about 1 *M*. At lower concentrations of quencher the apparent slope and hence the Stern–Volmer quenching constant is much less than that seen for the acrylamide quenching of Nile red bound to tubilin.[16] This implies that the probe is, on average, in a less accessible location within the matrix of HSA than in tubulin. It was also noted in the present work that at 0.2 *M* acrylamide, the peak emission of Nile red bound to HSA had shifted by ~2 nm toward the blue end of the spectrum, while in 2 *M* acrylamide the emission peak had shifted ~3 nm toward the red, relative to the aqueous probe–protein complex.

In general, the upward deviation in Fig. 2 implies a heterogeneity in the quenching mechanism, such as static and dynamic quenching. However, Fig. 3 shows no change in the lifetime decay components over this concentration range. This implies that there is no dynamic quenching occurring and hence all quenching is due to binding of acrylamide either to, or in the close proximity of, Nile red. Figure 4 shows the changes in the relative percentages of each decay component with quencher concentration. This further shows that there are at least two mechanisms for the quenching of probe on the protein. Initially, the longer decay components are much more easily quenched by acrylamide, and the relative contribution from these components to the total fluorescence decreases sharply with increasing acrylamide concentration to about 0.8 *M*.

At around 0.8 *M* acrylamide there is relatively very little unquenched long-lived excited state of Nile red. On

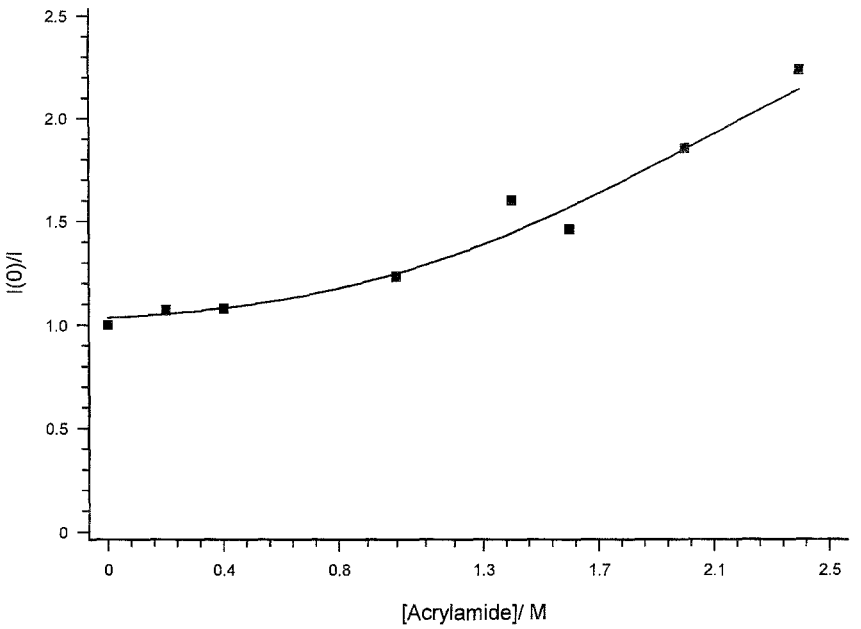

Fig. 2. Steady-state acrylamide quenching of Nile red bound to HSA in buffer (pH 7.1): a Stern–Volmer plot.

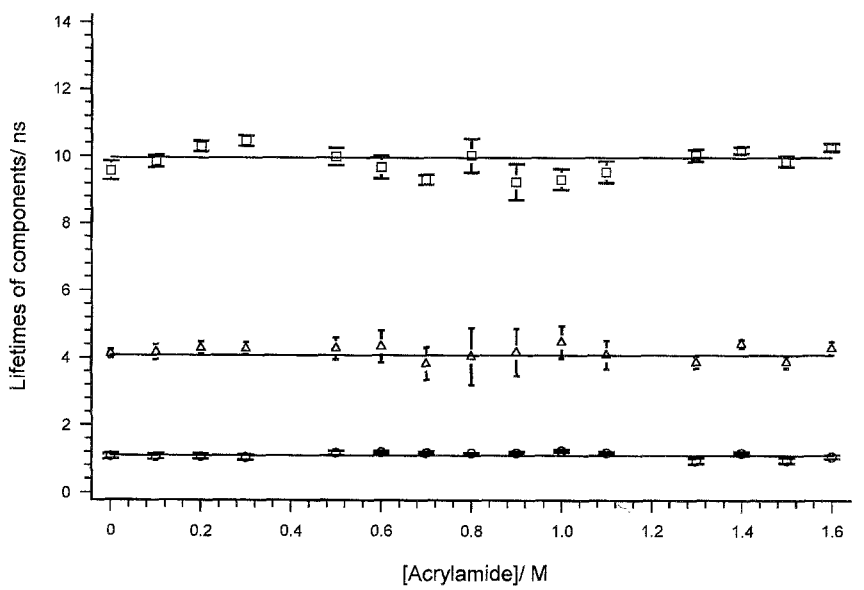

Fig. 3. Invariance of fluorescence decay components of Nile red bound to HSA in buffer (pH 7.1) on adding acrylamide.

the addition of around 1.3 *M* acrylamide there is almost-complete quenching of all Nile red molecules, and the relative distribution of lifetime components from unquenched excited states returns to uniform. Thus, the important question in hand is what could cause this heterogeneity in the acrylamide quenching of Nile red bound to HSA and hence the upward curvature to the steady-state Stern–Volmer plot.

It might be that the Nile red is bound in different sites within the protein matrix. This is consistent with the emission spectral shifts mentioned previously, if it is assumed that the emission of Nile red located in more exposed locations will be red-shifted from that of Nile red in more buried sites within the protein matrix. That is, at low acrylamide concentrations, Nile red in the more exposed binding sites is preferentially quenched

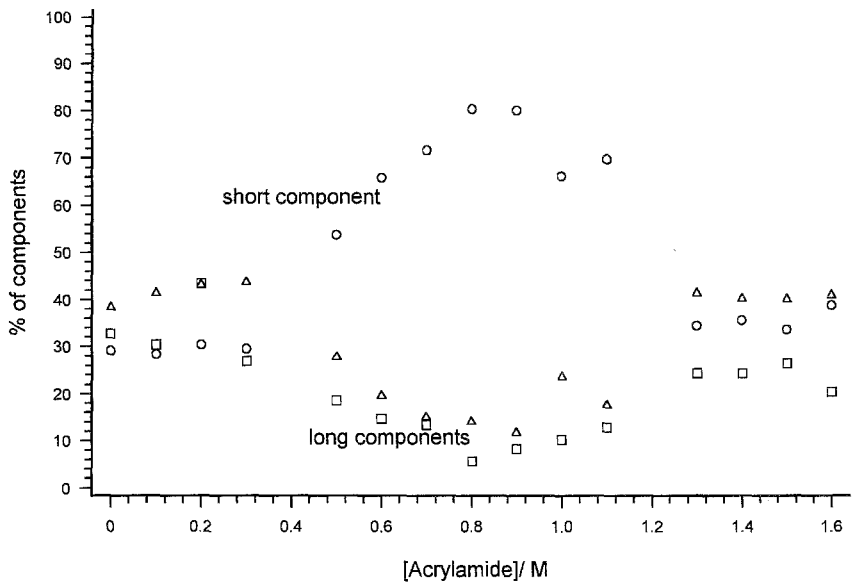

Fig. 4. Variation in relative percentages of the fluorescence decay components of Nile red bound to HSA with acrylamide concentration.

and a greater proportion of the fluorescence arises from the more buried sites. However, at much higher acrylamide concentrations some Nile red in the buried binding sites have been quenched, causing a shift in the emission back toward the red.

The fact that some of the long decay component is quenched in preference to a small amount of the shorter decay components (and the emission spectrum is red-shifted in 2 *M* acrylamide) implies that this analysis presented cannot be complete. The actual distribution of sites is more complex than this simple two-site model and/or the fluorescence decay of Nile red in each site is multiexponential, varying in the relative percentage of each decay component from site to site. However, this analysis of the acrylamide quenching results implies that the site of Nile red producing (a large proportion of) the long decay components is in a more polar (and hence more exposed) environment than the site of Nile red giving rise to the shorter decay component. This was not seen in the time-resolved emission spectra shown in Figure 1. This may be simply because the wavelength shifts between lifetime components are too small to be seen in Fig. 1.

However, another possible explanation of these unusual acrylamide quenching results is that at high quencher concentrations, there may be some weak binding of the quencher to the protein. In fact, it has been shown previously that acrylamide shows an unusually high degree of static quenching of the tryptophanyl fluorescence of HSA.[21] However, certainly at lower acrylamide concentrations, 0–0.8 *M*, there has been strong evidence to show that acrylamide does not bind to proteins.[22,23] An explanation of this unusually high degree of static quenching by acrylamide of the tryptophanyl fluorescence of HSA is that transient quenching effects may appear to contribute to the static quenching.[24] A further possible cause of the enhanced static quenching of Nile red at the high acrylamide concentrations used in this work is that some disruption to the protein's structure or dynamics may occur at these concentrations. That is, it may be that at high concentrations, such that there is approximately 1 acrylamide molecule present for every 25 water molecules, there is a disruption to the protein's native structure, caused by an alteration in the physical chemistry of the solvent.

There have been many studies of protein unfolding observed through steady-state fluorescence, producing some information regarding the changes in protein structure and dynamics (e.g., Ref. 1). However, it is usually very difficult to interpret such measurements of steady-state fluorescence in terms of precise changes in the protein's structure or dynamics. Nevertheless, measurements of the time-resolved fluorescence anisotropy of such transitions can give more direct information regarding both the structure and the dynamics of a protein.

Denaturant and many other solvents (and/or the impurities in commercially available samples) fluoresce in the same wavelength region as tryptophanyl emission and thus time-resolved fluorescence information is difficult to obtain by exploiting the intrinsic protein fluo-

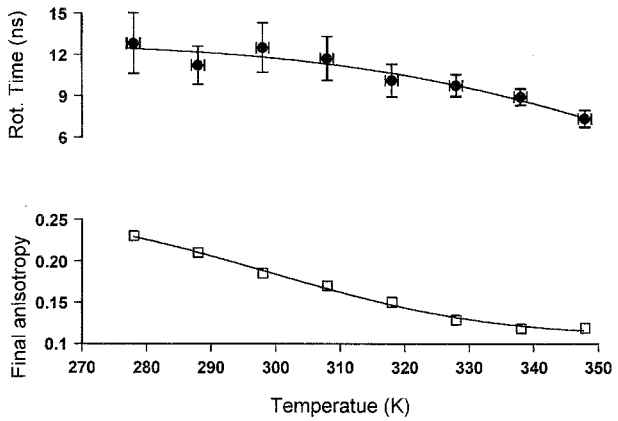

Fig. 5. Analysis of the time-resolved anisotropy decay of Nile red on HSA (aq.) at various temperatures.

rescence. Nevertheless, by using an extrinsic probe such as Nile red, time-resolved anisotropy measurements can reveal interesting structural and dynamic information for the protein, through observing changes in the rotational diffusion of the probe. Measurements of time-resolved fluorescence depolarisation (anisotropy) are generally analyzed in terms of three parameters; the initial anisotropy, r_0; the rotational correlation time, τ_r; and the final anisotropy, r_∞.[25] Respectively, these parameters relate to the intramolecular angular displacement between absorption and emission dipole moments, the diffusional rotation of the probe (as defined in the simplest case by the Stokes–Einstein equation), and the angle through which the probe is free to rotate in.[25] It is not obvious how the two latter parameters vary for a probe–protein complex as the protein is denatured. Figure 5 shows this information for Nile red bound to HSA.

The most striking feature about Fig. 5 is that there is no change in either parameter to signal the unfolding transition at a specific temperature. Moreover, there is a gradual decrease in both the rotational time and the final anisotropy, the latter of which levels off by about 330 K. This implies that on increasing temperature, both the speed of rotational diffusion and the angular size of the cone in which the probe can rotate, steadily increase, at least until 330 K. Furthermore, the peak emission wavelength of the probe was found to remain constant at ~639 nm throughout the temperature range 278–343 K.

This is in contrast to the relatively sharp unfolding transition seen in Fig. 6 as a shift in the peak emission wavelength of the intrinsic tryptophanyl fluorescence at around 320 K. A similarly sharp change in the secondary structure of the protein at approximately 320 K can be seen in the temperature variation of the circular dichroism of HSA in phosphate buffer of pH 7.4.[26] However, the fluorescence spectroscopic analysis of Nile red bound to HSA reported here implies that the protein matrix about the site of the extrinsic probe moves through a continuous change in dynamical freedom with increasing temperature, in contrast to the sharp change in protein structure about the tryptophanyl residue seen at the unfolding temperature.

Furthermore, the constancy in the steady-state emission of the extrinsic probe with increasing temperature implies that the probe remains in a hydrophobic environment within the unfolded protein matrix. This is strong evidence that the nature of the unfolded protein cannot be approximated to a random coil in which the extrinsic probe would become exposed to an aqueous environment. This is consistent with the view that hydrophobic regions of HSA are not unfolded as easily as the helical content of the protein.[27] In fact, the tryptophanyl emission spectrum of the thermally denatured protein reported here is closer to that of the disulfide-reduced state of HSA rather than the denatured reduced form.[28]

In contrast, unfolded protein in both urea and guanidine hydrochloride shifts the peak emission from bound Nile red to around 660 nm and significantly lowers the fluorescence intensity. In fact, the emission from bound Nile red is reduced by about 50% in 2 *M* urea relative to the aqueous solution. This is strong evidence that the environment of Nile red bound to unfolded HSA is distinct for thermally denatured protein and that denatured by guanidine or urea. In particular, this implies that Nile red remains buried in a hydrophobic location within thermally denatured HSA, whereas it becomes exposed to a polar environment when bound to HSA denatured by guanidine or urea. This is consistent with the structure of the unfolded protein in denaturant being distinct from the structure of the protein that is thermally denatured. In fact, the results reported here suggest that some elements of the secondary structure of HSA remain intact upon heating to 340 K, whereas they are completely unfolded by denaturant. For example, it is possible that the thermally denatured protein at ~320 K is a disulfide-reduced form of HSA, whereas the chemically denatured protein is more completely unfolded.

Figure 7 shows the variation in rotational correlation time, τ_r, with concentration of denaturant using both urea and guanidine hydrochloride. This shows an increase in the speed of rotational diffusion with increasing denaturant concentration. As expected, the effects are more pronounced with guanidine hydrochloride, as this is commonly observed to be the more powerful denaturant. Figure 8 shows the change in final anisotropy

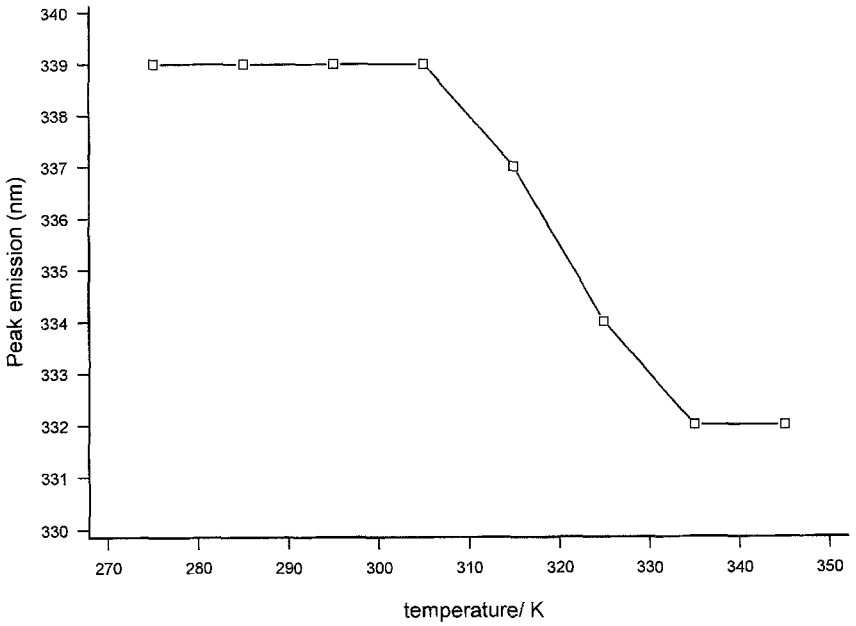

Fig. 6. Thermal unfolding of HSA seen as the variation in Stokes shift of the intrinsic tryptophanyl fluorescence.

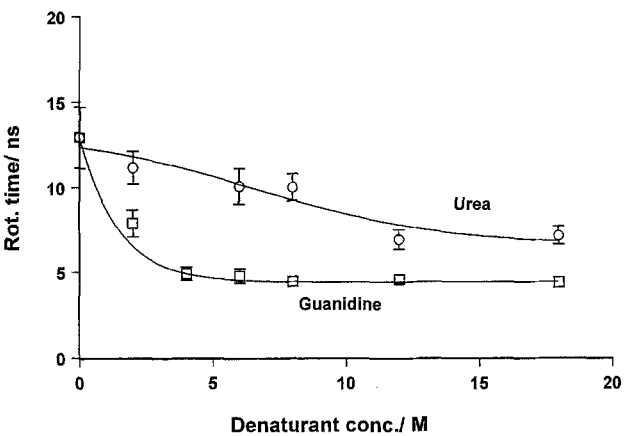

Fig. 7. Variation in rotational correlation time for Nile red on HSA with denaturant concentration for urea and guanidine hydrochloride.

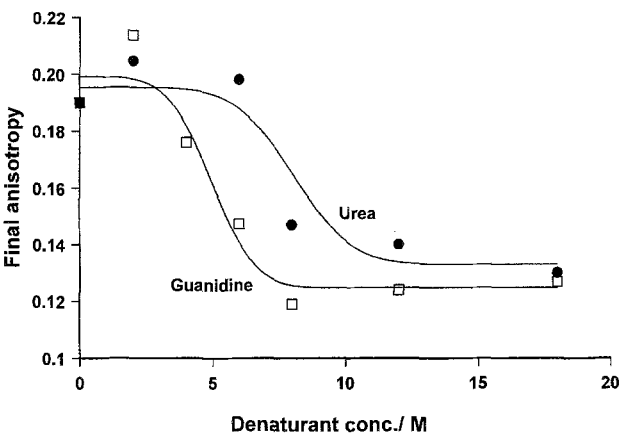

Fig. 8. Variation in final anisotropy with denaturant concentration for urea and guanidine hydrochloride.

of the bound probe with increasing denaturant concentration. This shows that there is a sharp decrease in the final anisotropy at the unfolding transition, as opposed to the gradual change seen with thermal unfolding. As expected, this transition occurs at a lower concentration for guanidine than for urea. Thus, with regard to the angular size of the cone for which the bound probe can rotate in, there is a relatively sudden increase at the unfolding denaturant concentration. This is in contrast to a gradual increase with increasing temperature over the range of temperatures chosen. This demonstrates that unfolding by heating and by denaturant can also be distinguished, in respect of protein dynamics.

Reverse micelles are spontaneously formed systems with surfactant molecules separating a waterpool from a bulk organic phase. The waterpool size of the reverse micelle is varied by simply injecting more or less water into the solution and is denoted by the molar ratio of water to surfactant present, ω_0.[29] Our previous work has demonstrated that compartmentalized proteins in reverse micelles may have an induced conformational stability when the reverse micelle is of specific waterpool

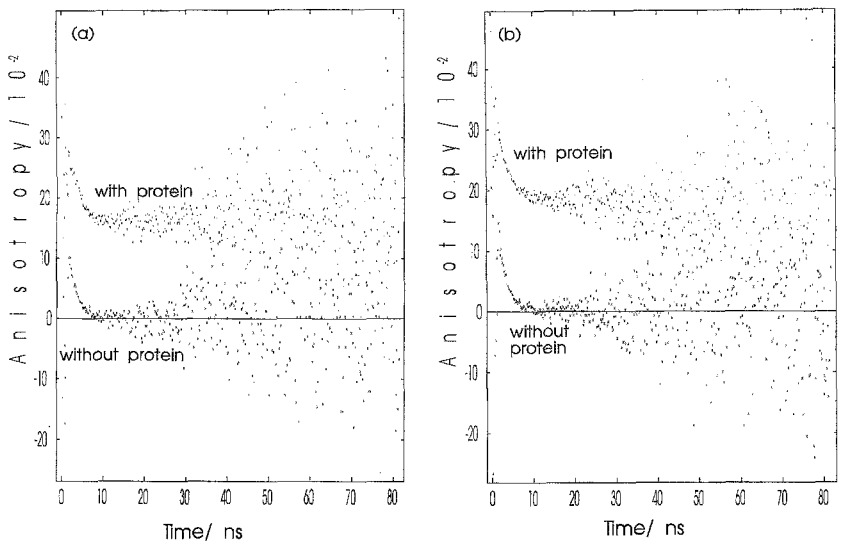

Fig. 9. Time-resolved anisotropy of Nile red in reverse micelles in the presence and absence of protein. Reverse micelles are made of isooctane and Trizma buffer (pH 7.1) with (a) the anionic surfactant AOT or (b) the cationic surfactant CTAC. In a, the molar ratio of water to surfactant (ω_0) is 30, while in b, ω_0 = 70.

size.[9,10] This induced conformational stability was found to occur, for HSA, at ω_0 = 21.[9,10] Thus, having characterized the fluorescence properties of Nile red bound to HSA above, we can return to our original motivation for this study, namely, further investigation into the nature of HSA compartmentalized in reverse micelles.

Two types of surfactant were used here, the commonly used anionic surfactant AOT and the less used cationic surfactant CTAC. Figure 9 shows the time-resolved anisotropy of Nile red in both (a) AOT and (b) CTAC reverse micelles in the presence and absence of protein. In the case of the protein being present, the Nile red and protein solution were mixed prior to incorporation into the micellar solution. The obvious feature of these traces is that the final anisotropy of the probe–protein complex remains high (~0.2) in both cases where the protein is present. This clearly demonstrates that the probe remains bound to the protein and does not partition into the isooctane phase. In the case of AOT reverse micelles, there was no significant change in final anisotropy with increasing waterpool size in the ω_0 range 12 to 36.

However, reconvolution of the data to retrieve a single rotational correlation time proved to be difficult.

Figure 10 shows the changes in steady-state fluorescence of Nile red bound to HSA in AOT/isooctane/buffer reverse micelles with increasing waterpool size. This is reminiscent of similar trends seen in the changes in the fluorescence of *N*-acetyl-tryptophanamide (NATA) reported previously.[10,30] The results presented here show

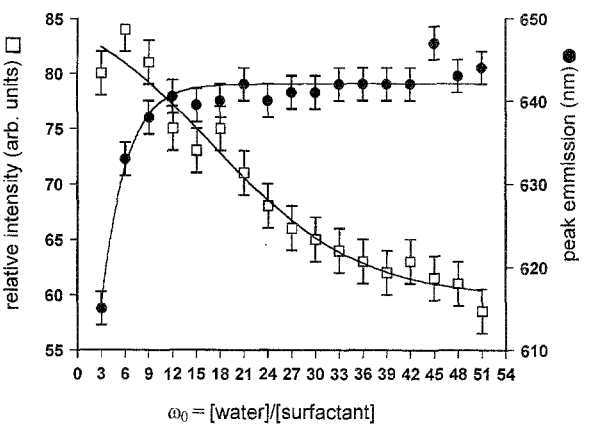

Fig. 10. Steady-state fluorescence analysis of Nile red bound to HSA in AOT reverse micelles with increasing waterpool size.

that the environment of the probe becomes more polar with increasing waterpool size. Since the probe remains bound to the protein at all waterpool sizes (see above), this implies that the protein moves into a more polar environment with increasing waterpool size. This is the same interpretation given to the similar behavior of NATA[10,30] and implies that, in general, molecules incorporated in reverse micellar systems are in a more aqueous environment at higher waterpool sizes. However, this is in contrast to the consistent peak emission seen in the intrinsic tryptophan fluorescence of HSA in reverse micelles with increasing waterpool size. This is

probably because the tryptophan residue lies in a hydrophobic pocket[31] which shields it somewhat from environmental changes caused to the protein.

CONCLUSIONS

We have demonstrated how complementary information can be retrieved from the fluorescence spectroscopy of extrinsic probes regarding protein structure and dynamics, with the specific example of Nile red and human serum albumin.

In particular, we have shown the following.

(a) Protein unfolding in denaturant and that by heating have very different effects on the conformation and dynamics of HSA.

(b) HSA in reverse micelles lies in a more aqueous environment at larger waterpool sizes, which was previously not seen in experiments exploiting the intrinsic protein fluorescence.

(c) There is some heterogeneity in the static acrylamide quenching of Nile red bound to HSA, the precise nature of which we have not elucidated.

We are currently investigating the acrylamide quenching of the Nile red–protein complex in reverse micelles at various waterpool sizes (preliminary results are reported in Ref. 32), to investigate further the induced conformational stability around $\omega_0 = 21$, previously observed in studies exploiting the tryptophanyl fluorescence of HSA.[10]

ACKNOWLEDGMENTS

The use of reverse micelles was inspired by our industrial collaborators at Zeneca, namely, Rod Kittlety, Paul Gellert, and Rod Swart, and builds on earlier work carried out by David McLoskey at Stratclyde University. We would also like to acknowledge helpful discussions with David Hatrick and Graham Hungerford. D.M.D. is funded by a CASE EPSRC award with ICI/Zeneca.

REFERENCES

1. T. E. Creighton (1993) *Proteins: Structure and Molecular Properties*, W. H. Freeman, New York.
2. M. R. Eftink (1994) *Biophys. J.* **66**, 482–501.
3. J. B. A. Ross and M. R. Eftink (1992) *SPIE Proc.* **1640**, 2–9.
4. J. M. Beechem and L. Brand (1985) *Annu. Rev. Biochem.* **54**, 43–71.
5. C. J. Smith, A. R. Clarke, W. N. Chia, L. I. Irons, T. Atkinson, and J. J. Holbrook (1991) *Biochemistry* **30**, 1028–1036.
6. M. R. Otto, M. P. Lillo, and J. M. Beechem (1994) *Biophys. J.* **67**, 2511–2521.
7. D. J. S. Birch, D. McLoskey, A. Sanderson, K. Suhling, and A. S. Holmes (1994) *J. Fluoresc.* **4**(1), 91–102.
8. M. Ameloot, N. Boens, R. Andriessen, V. Vandenbergh, and F. C. DeSchryver (1992) in L. Brand and L. Johnson (eds.), *Methods in Enzymology, Vol. 210. Numerical Computer Methods*, Academic Press, San Diego, pp. 314–340.
9. D. M. Davis, D. McLoskey, D. J. S. Birch, R. M. Swart, P. R. Gellert, and R. S. Kittlety (1994) *SPIE Proc.* **2137**, 331–342.
10. D. M. Davis, D. McLoskey, D. J. S. Birch, P. R. Gellert, R. S. Kittlety, and R. M. Swart *Biophys. Chem.* (in press).
11. D. Basting, D. Ouw, and F. P. Schäfer (1976) *Opt. Comm.* **18**(3), 260–262.
12. W. J. Brown, T. R. Sullivan, and P. Greenspan (1992) *Histochemistry* **97**, 349–354.
13. S. D. Fowler and P. Greenspan (1985). *J. Histochem. Cytochem.* **33**(8), 833–836.
14. J.-R. Daban, M. Samsó, and S. Bartolomé (1991) *Anal. Biochem.* **199**, 162–168.
15. D. L. Sackett and J. Wolff (1987) *Anal. Biochem.* **167**, 228–234.
16. D. L. Sackett, J. R. Knutson, and J. Wolff (1990) *J. Biol. Chem.* **265**(25), 14899–14906.
17. P. Greenspan and P. Lou (1993) *Int. J. Biochem.* **25**(7), 987–991.
18. D. J. S. Birch and R. E. Imhof (1981) *Rev. Sci. Instrum.* **52**, 9–15.
19. G. Hungerford (1991) *Ph.D. thesis*, Strathclyde University, Glasgow, UK.
20. J. R. Lakowicz (1983) *Principles of Fluorescence Spectroscopy*, Plenum Press, New York.
21. M. R. Eftink and C. A. Ghiron (1976) *Biochemistry* **15**(3), 672–681.
22. M. R. Eftink and C. A. Ghiron (1987) *Biochim. Biophys. Acta* **916**, 343–349.
23. D. H. Tallmadge, J. S. Huebner, and R. F. Borkman (1989) *Photochem. Photobiol.* **49**(4), 381–386.
24. M. R. Eftink (1991) in J. R. Lakowicz (Ed.), *Topics in Fluorescence Spectroscopy, Vol. 2. Principles*, Plenum Press, New York, pp. 53–126.
25. R. F. Steiner (1991) in J. R. Lakowicz (Ed.), *Topics in Fluorescence Spectroscopy. Vol. 2. Principles*, Plenum Press, New York, pp. 1–52.
26. Z. Kranjc, S. Lapanje, and N. Poklar (1994) *Acta Chim. Slovenica* **41**(3), 279–294.
27. J. Chmelík, P. Anzenbacher, J. Chmelíková, M. Matejckova, and V. Kalous (1988) *Collect. Czech. Chem. Commun.* **53**, 411–422.
28. J. Y. Lee and M. Hirose (1992) *J. Biol. Chem.* **267**(21), 14753–14758.
29. K. Kalyanasundaram (1987) *Photochemistry in Microheterogeneous Systems*, Academic Press, London.
30. S. Ferreira and E. Gratton (1990) *J. Mol. Liq.* **45**, 253–272.
31. X. M. He and D. C. Carter (1992) *Nature* **358**, 209–215.
32. D. M. Davis, D. J. S. Birch, R. M. Swart, P. R. Gellert, and R. S. Kittlety (1995) *SPIE Proc.* **2388**, 302–313.